Original Article
Bulletin of Pure and Applied Sciences.
Chemistry , Vol.42 C, No.1
January-June 2023: P.14-21

http://www.bpasjournals.com/chemistry
DOI: 10.48165/bpas.2023.42C.1.3
Print version ISSN 0970 4620
Online version ISSN 2320 320X

Sunlight Induced Photocatalytic Degradation of Methylene Blue Dye by SnS_2 Nanoplates Under Natural Sunlight Exposure

[1]Gajendra Kumar* and [2]Alok Kumar Gehlot

Author Affiliations
[1]Department of Chemistry, Constituent Government College (MJPRU), Hasanpur, Amroha, Uttar Pradesh 244241, India
[2]Department of Mathematics, Faculty of Engineering, Teerthanker Mahaveer University, Moradabad, Uttar Pradesh 244001, India

***Corresponding Author**
Gajendra Kumar, Department of Chemistry, Constituent Government College (MJPRU), Hasanpur, Amroha, Uttar Pradesh 244241, India
E-mail: gaj.chem@gmail.com, gandhravk.engineering@tmu.ac.in

Received on 27.12.2022, Revised on 07.02.2023, Approved on 09.04.2023, Accepted on 15.04.2023, Published on 20.06.2023

ABSTRACT
Removal of dyes from water bodies is a significant concern throughout the world. In this study, SnS_2 nanoplates were synthesized by a hydrothermal synthetic route at 160°C, and it is effectively characterized by various techniques. The XRD peaks confirmed the hexagonal planes of SnS_2. The nanoplates-like morphology was revealed by FESEM and HRTEM. The optical band gap was investigated by UV-vis DRS and showed a reflection edge with corresponding energy at 2.2 eV. The photocatalytic activity of the SnS_2 nanoplates is tested against the degradation of methylene blue under natural sunlight irradiation. About 95% degradation of methylene blue is observed in 120 min with the photocatalytic degradation rate of $0.021 min^{-1}$. Results confirmed that the SnS_2nanoplatescould facilitate 95 % degradation of methylene dye and followed the first-order kinetic model.

Keywords: SnS_2; Solar Photocatalyst; Methylene Blue, Photocatalysis

How to cite this article: Kumar G. and Gehlot A.K. (2023). Sunlight Induced Photocatalytic Degradation of Methylene Blue Dye by SnS_2 Nanoplates Under Natural Sunlight Exposure. *Bulletin of Pure and Applied Sciences-Chemistry,* 42C (1), 14-21.

INTRODUCTION

Extensive usage of organic dyes in textile and other fabric industries leads to the contamination of water bodies (Homem & Santos, 2011; Qin et al., 2021; Rivera-Utrilla et al., 2013). A large number of water sources are polluted by residual dyes, which enter directly into the aquatic environment through various means like dye industries, textile industries, etc. (Dinh et al., 2017; Michael et al., 2013). As a cationic dye methylene blue found its wide application in coloring fabrics. Due to its water-soluble nature, methylene blue is highly stable in an aquatic environment, non-biodegradable, and cancer-causing in nature, which makes it harmful to humans and living species of aquatic ecosystems.

However, due to their highly stable nature in water, these residual dyes are not quickly metabolized, as a result of which they can easily pollute groundwater and surface water, causing harmful diseases in animals and humans. To date, several methodologies have been used for wastewater remediation, but they have certain

drawbacks such as excessive sludge formation, and other harmful byproducts generation. In order to overcome these limitations, semiconductor-based photocatalysts are widely utilized for the photocatalytic removal of various water pollutants (Akbari et al., 2021; Calvete et al., 2019; Durán-Álvarez et al., 2016). To date, zinc oxide and titanium dioxide nanoparticles are the most used photocatalysts for degrading organic dyes, but they require ultraviolet light for photoexcitation as their band gap is large. Recently, over the last few decades, tin-based photocatalysts have beenutilized as the most promising and new class of photocatalysts for wastewater treatment. The tin-based photocatalyst found applications in various areas such as the production of ammonia from nitrogen, water-splitting, reduction of CO_2, and degradation of water pollutants through heterogeneous photocatalysis. The band structure of these materials provides them with a suitable band gap for visible light-active and a well-distributed valence band in favor of recombination charge, enabling them to act as potential photocatalytic materials for wastewater treatment over metal oxides. Another class of heterogeneous semiconductors photocatalysts is metal sulfides, which mostly utilize the light in the visible region and work in the small wavelength region i.e., (NIR) near-infrared regions. This light harvesting property make them a suitable visible light driven photocatalysts. The band gap of SnS_2 ranges between 1.8-2.3 eV, beside this is considered to be non-toxic, less costly, and has phenomenal chemical stability in neutral and acidic medium(Zhang et al., 2011). Because of all these properties SnS_2 is considered an efficient visible and NIR light-active photocatalyst. For an effective photocatalytic reaction in visible light, a semiconductor photocatalyst must possess a narrow band gap, with a low charge recombination rate, with conduction band on more negative potential side and valence band on positive potential side(Wang et al., 2014).

Synthesis of SnS_2 nanoplates

4.0 milli mole $SnCl_4.5H_2O$ was added into the50 milli litre of distilled water, then 8 milli mole of thiourea was slowly added into it followed by a continuous mixing with the help of magnetic stirrer, until a clear homogenous solution was prepared. Finally, after constant stirring of 45 min, the mixture was poured into a autoclave and heated at a temperature of 160°C for 24 h. The finally prepared precipitates were washed with DI water and C_2H_5OH and separated by centrifugation for 20 min at 7000 rpm, and the yellow material finally obtained was dried in an oven at 50°C.

Methodology for photocatalytic experiment

The photocatalytic performance of the SnS_2photocatalyst was determined by observing the degradation of methylene blue dye (20 mg/L) solutions under exposure to natural sunlight radiation. Typically, a 100 mL aqueous solution of 20 ppm methylene blue dye is taken into a 500 mL beaker, followed by the addition of 60 mg of SnS_2photocatalysts into it, which was then subjected to continuous stirring for 60 min under the dark condition. After 60 min of dark study, the beaker was kept under sunlight. 2 mL aliquot was taken from the beaker at certain intervals. The change in concentration of the MB molecule was monitored by UV-vis spectrophotometer at absorbance λ= 664 nm.

RESULTS AND DISCUSSIONS

XRD analysis

The XRD spectra of pristine SnS_2 were investigated by Bruker AXS advanced diffractometer with a scan range of 1 min^{-1} using graphite monochromatized Cu Kα radiation (1.5418 Å) operated at 40kilovolts. The XRD peaks for SnS_2 were detected at2θ = 2θ=14.9°, 28.4°, 32.2°, 33.6°, 46.3°, 49.7° and 52.7°which are matched to (0 0 1), (1 0 0), (0 0 2), (1 0 1), (0 0 3), (1 1 0) and (1 1 1)hexagonal planes of SnS_2(Card No.- 89-1758) (Figure.1). The lattice parameters are calculated to be as *a* = 3.61Å, *b* = 3.61Å, and *c* =6.82 Å, with the average crystallite size of 14.20 nm.

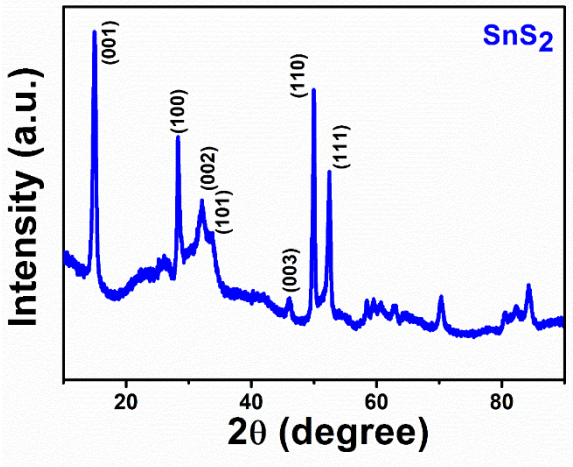

Figure1: XRD patterns of as-synthesized SnS_2 nanoplates

FE-SEM and HR-TEM analysis of SnS_2

The SnS_2 photocatalyst surface morphology was investigated by electron microscopy. The FE-SEM image of SnS_2 nanoplates was recorded by Zeiss FESEM, Ultra-plus55shows nanoplate-like structures with a diameter in the range of 250-500 nm (Figure. 2a and 2b). Similarly, the morphology of the SnS_2 nanoplates was better displayed from the HRTEM images with their corresponding SAED pattern (Figure. 2c-d and 2e) recorded on a JEM-3200FS, JEOL transmission electron microscope.

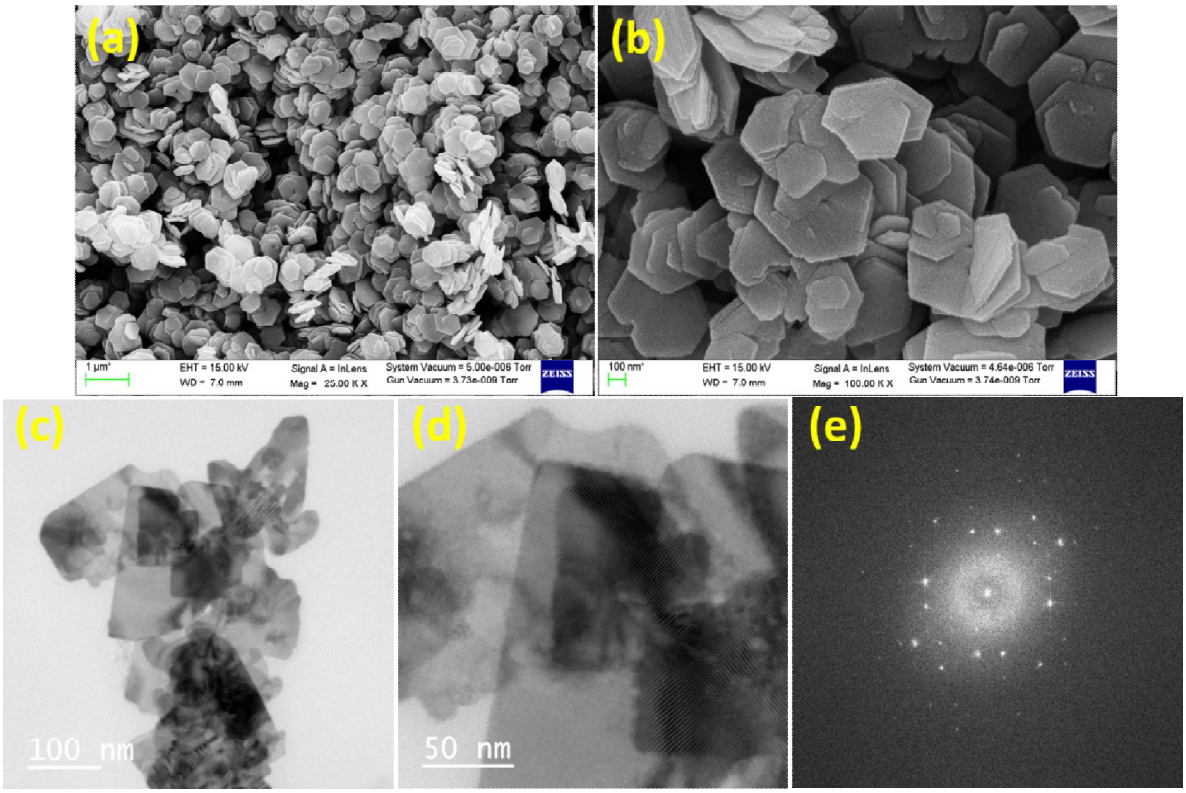

Figure 2: (a-b) FE-SEM image of SnS_2 nanoplates; (c-d)HR-TEM image of SnS_2 nanoplates and, (e) SAED pattern of SnS_2 nanoplates

Band gap analysis

The UV-vis DRS studies of the as-preparedSnS_2 nanoplates were recorded on a Shimadzu UV-2450, Japan spectrophotometer using $BaSO_4$ as a reference. The pure SnS_2 nanoplates absorb in the ultraviolet and visible light region (Figure 3a). The UV-vis DRS spectra were changed into absorption spectra by using (K-M function) Kubelka-Munk (Kortüm, 1969), and the band gap was calculated from the Taucs plots (Tauc et al., 1966), Figure 3 shows Tauc's plots of SnS_2 photocatalyst. The optical band gap of SnS_2 was determined to be 2.2 eV.

$$(\alpha h\nu)^{1/n} = A(h\nu - E_g) \quad (1)$$

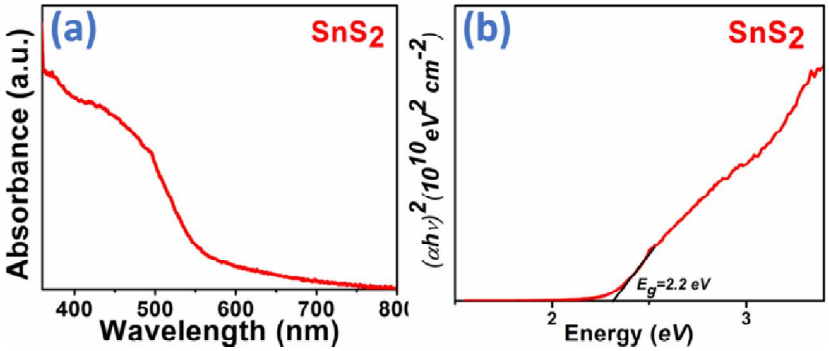

Figure 3: (a) UV-vis DRS spectra of SnS_2; (b) Tauc's plot of pure SnS_2

Photocatalytic activity

The impact of photocatalyst dose on the photocatalytic performance was investigated by treating the aqueous solution MB with different amounts of photocatalyst, i.e., 40–80 mg of photocatalyst per 100mL under the same experimental environment as mentioned above. The degradation rate and removal efficiency were first increased with the increase in the photocatalyst dose from40 mg (k=0.005 min^{-1}) to 60 mg/100mL (k=0.021 min^{-1}) and then decreased for the dose 80 mg (k=0.012 min^{-1}) (Figure.4a and 4b). The impact of the change in concentration of MB solution has been investigated by changing the initial concentration of MB solution from20 to 40 mg/L. The decrease in the photocatalytic performance was observed with the increase in MB concentrations (Figures. 4c and 4d). A complete photocatalytic degradation study was performed with a photocatalyst dose of 60 mg per 100 mL aqueous solution of MB.

The sunlight-mediated photocatalytic degradation of MB dye (20 mg/L) by the SnS_2 nanoplates is shown as a curve of C_t/C_0 vs. (t) time (Figure 4). In the dark experiment firstly, the change in concentration of MB dye was determined by the adsorption experiment. Roughly 36% of MB dye was adsorbed over SnS_2 nanoplates (Figure. 4a). The self-decomposition investigation of methylene blue shows negligible results. The SnS_2nanoplates show the photocatalytic performance of about 95 % methylene blue dye degradation after 150 min of sunlight exposure. The degradation kinetics of methylene blue was modelled by a 1st-order kinetics model. The 1storder kinetics equation is:

$$\ln(C_0/C_t) = kt \quad (2)$$

Where C_0 is the initial dye concentration of dye, and C_t is the dye concentration at any time, whereas k (min^{-1}) (Table 1) is the 1st-order kinetic rate constant for MB dye photocatalytic degradation. The photocatalytic rate constant of pristine SnS_2 (k= 0.021 min^{-1}) (Figure 4b). Figure.4c shows the UV-vis absorption spectra, which shows the change in concentration of methylene blue dye during the photocatalytic degradation. The decrease in the intensity of the absorption peak of methylene blue dye (664 nm) was observed over 120 min period of sunlight irradiation.

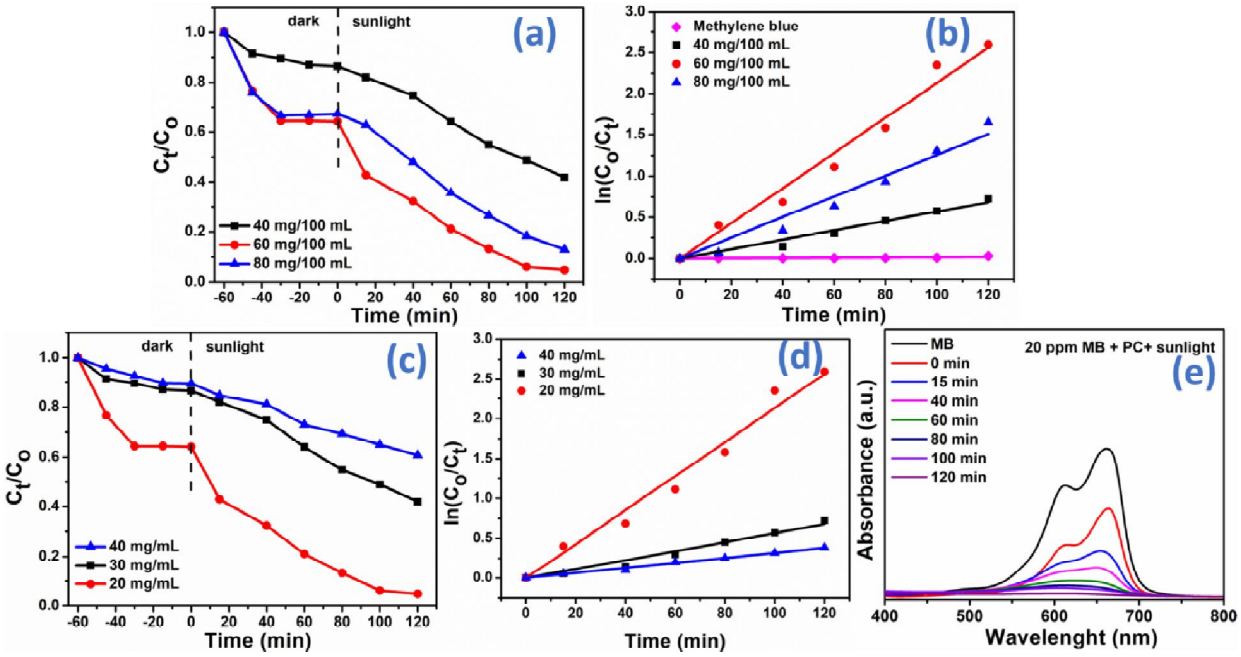

Figure 4: (a)Effect of photocatalyst dose on the photocatalytic performance, (b) Corresponding 1st order kinetics curves, (c) Effect of MB dye concentration on the photocatalytic performance, (d) Corresponding 1st order kinetic curves, e) UV-is absorbance spectra of MB dye solution.

Table1: Summary of kinetics study of MB dye photocatalytic degradation

Sample name	**Percentage Adsorption**	**Percentage Degradation**	**1st-order kinetics (MB)**	
			***k* (Min^{-1})**	**R^2**
SnS_2	36%	95%	0.021	0.985
Blank	NA	10%	0.001	0.993

Chemical stability of photocatalyst

The chemical stability of the used SnS_2photocatalyst was confirmed by the XRD pattern and FESEM images obtained after the 3rd cycle (Figure. 5a and 5b).

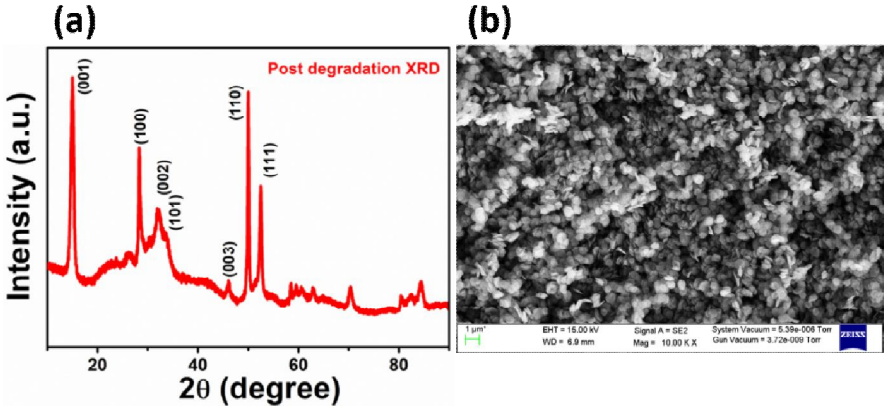

Figure 5: (a) Post degradation XRD and (b) SEM image of the re-used photocatalyst.

Reactive oxygen species (ROS) scavenging studies

The main radical responsible for the photocatalytic degradation of methylene blue is determined by the ROS experiment, the radical scavenging experiment was performed in the presence of (1mM) ammonium oxalate (h^+), (1mM) chloroform (O_2^{-}•scavenger) and (1mM) isopropyl alcohol (OH• scavenger) respectively, under the optimized conditions. The radical scavenging experiment confirmed that the O_2^{-}• radical and photogenerated holes are the main active species which involve in the photocatalytic degradation processes of methylene blue (MB) (Figure 6).

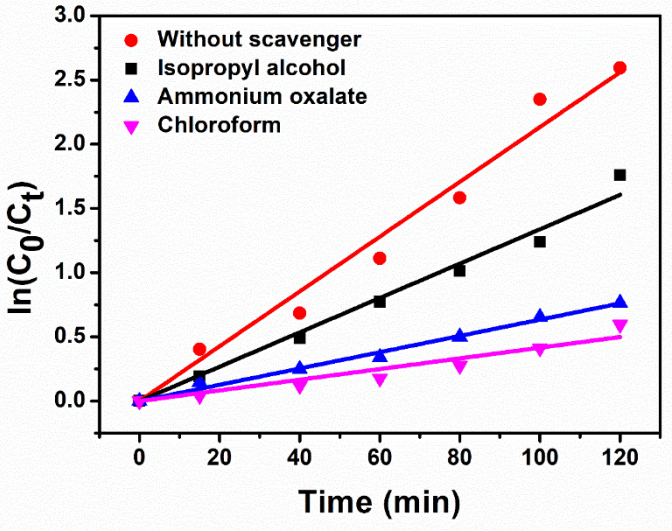

Figure 6: Effect of reactive oxygen species on MB degradation

Photocatalytic mechanism

In the semiconductor photocatalyst, the charge transfer mainly depends on the place of the conduction and valence band on the NHE scale. The conduction and valence band potential values are calculated by the equation, $ECB = \chi(AaBb) - 1/2Eg + E0$ and $EVB = ECB+Eg$ (Reddy et al., 1998) where band gap ofSnS_2isrepresents by *Eg*, the value of conduction band potential is represented by ECB, whereas the potential value of the valence band is represented by EVB, and *E0* value is taken as – 4.50 eV, *i.e.*, the energy of free electrons on the NHE scale. The value χ (AaBb) represents the absolute electronegativity of a semiconductor material of the AaBb type. For SnS_2, the electronegativity value is calculated to be 6.55 eV. Upon exposure to visible light radiation, the electron excited from the valance band into the conduction band. The conduction and valence bands of SnS_2 are calculated as –0.95eV and +1.28eV, respectively. The valance band of SnS_2 was estimated to be +2.2eV (vs. NHE), which has been more negative potential value than that of $OH^{\bullet}/H_2O$ (+1.08 eV vs. NHE), which confirm that the photo-generated holes are capable to oxidize water to yield hydroxyl ($OH^{\bullet}$) radicals in SnS_2. The conduction band potential of SnS_2 was estimated to be (–0.95eV vs. NHE),which is more negative than $E(O_2/O_2^{-}\bullet)$ (–0.04 eV vs. NHE) (Li et al., 2018), so it can quickly reduce O_2 to produce superoxide radical O_2^{-}•.

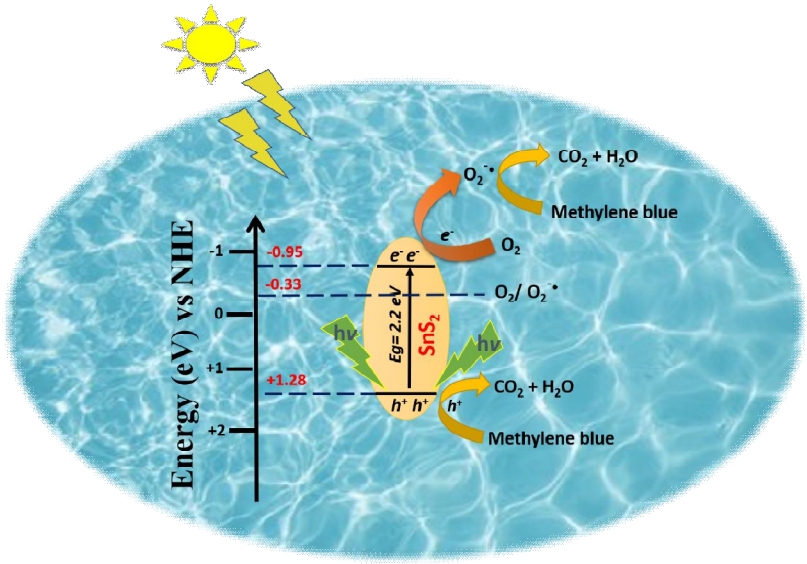

Figure 7: The proposed photocatalytic mechanism over SnS_2 under sunlight irradiation

CONCLUSIONS

A simple hydrothermal synthetic route has been used for the synthesis of SnS_2 photocatalyst. The SnS_2 photocatalyst shows excellent photocatalytic performance towards the degradation of 95% of methylene (MB) under sunlight irradiation. The corresponding kinetic rate constant of the SnS_2 photocatalyst was 0.021 min^{-1}. SnS_2 is an effective visible light photocatalyst option for removing various organic dyes in aqueous media due to its strong photocatalytic activity.

REFERENCES

1. Akbari, M. Z., Xu, Y., Lu, Z., & Peng, L. (2021). Review of antibiotics treatment by advance oxidation processes. *Environmental Advances*, *5*, 100111. https://doi.org/10.1016/j.envadv.2021.100111
2. Calvete, M. J. F., Piccirillo, G., Vinagreiro, C. S., & Pereira, M. M. (2019). Hybrid materials for heterogeneous photocatalytic degradation of antibiotics. *Coordination Chemistry Reviews*, *395*, 63–85. https://doi.org/10.1016/j.ccr.2019.05.004
3. Dinh, Q. T., Moreau-Guigon, E., Labadie, P., Alliot, F., Teil, M. J., Blanchard, M., & Chevreuil, M. (2017). Occurrence of antibiotics in rural catchments. *Chemosphere*, *168*, 483–490. https://doi.org/10.1016/j.chemosphere.2016.10.106
4. Durán-Álvarez, J. C., Avella, E., Ramírez-Zamora, R. M., & Zanella, R. (2016). Photocatalytic degradation of ciprofloxacin using mono- (Au, Ag and Cu) and bi- (Au-Ag and Au-Cu) metallic nanoparticles supported on TiO2 under UV-C and simulated sunlight. *Catalysis Today*, *266*, 175–187. https://doi.org/10.1016/j.cattod.2015.07.033
5. Homem, V., & Santos, L. (2011). Degradation and removal methods of antibiotics from aqueous matrices - A review. *Journal of Environmental Management*, *92*(10), 2304–2347. https://doi.org/10.1016/j.jenvman.2011.05.023
6. Kortüm, G. (1969). *Reflectance Spectroscopy, translated by JE Lohr*. Springer Verlag, New York.
7. Li, C., Yu, S., Dong, H., Liu, C., Wu, H., Che, H., & Chen, G. (2018). Z-scheme mesoporous photocatalyst constructed by modification of Sn3O4 nanoclusters on g-C3N4 nanosheets with improved photocatalytic performance and mechanism insight. *Applied Catalysis B: Environmental*, *238*(July), 284–293. https://doi.org/10.1016/j.apcatb.2018.07.049
8. Michael, I., Rizzo, L., McArdell, C. S.,

Manaia, C. M., Merlin, C., Schwartz, T., Dagot, C., & Fatta-Kassinos, D. (2013). Urban wastewater treatment plants as hotspots for the release of antibiotics in the environment: A review. *Water Research*, *47*(3), 957–995. https://doi.org/10.1016/j.watres.2012.11.027

9. Qin, K., Zhao, Q., Yu, H., Xia, X., Li, J., He, S., Wei, L., & An, T. (2021). A review of bismuth-based photocatalysts for antibiotic degradation: Insight into the photocatalytic degradation performance, pathways and relevant mechanisms. *Environmental Research*, *199* (March), 111360. https://doi.org/10.1016/j.envres.2021.111360

10. Reddy, R. R., Nazeer Ahammed, Y., Rama Gopal, K., & Raghuram, D. V. (1998). Optical electronegativity and refractive index of materials. *Optical Materials*, *10*(2), 95–100. https://doi.org/10.1016/S0925-3467(97)00171-7

11. Rivera-Utrilla, J., Sánchez-Polo, M., Ferro-García, M. Á., Prados-Joya, G., & Ocampo-Pérez, R. (2013). Pharmaceuticals as emerging contaminants and their removal from water. A review. *Chemosphere*, *93*(7), 1268–1287. https://doi.org/10.1016/j.chemosphere.2013.07.059

12. Tauc, J., Grigorovici, R., & Vancu, A. (1966). Optical Properties and Electronic Structure of Amorphous Germanium. *Physica Status Solidi (B)*, *15*(2), 627–637. https://doi.org/https://doi.org/10.1002/pssb.19660150224

13. Wang, H., Zhang, L., Chen, Z., Hu, J., Li, S., Wang, Z., Liu, J., & Wang, X. (2014). Semiconductor heterojunction photocatalysts: Design, construction, and photocatalytic performances. *Chemical Society Reviews*, *43*(15), 5234–5244. https://doi.org/10.1039/c4cs00126e

14. Zhang, Y. C., Du, Z. N., Li, K. W., Zhang, M., & Dionysiou, D. D. (2011). High-performance visible-light-driven SnS2/SnO2 nanocomposite photocatalyst prepared via in situ hydrothermal oxidation of SnS2 nanoparticles. *ACS Applied Materials and Interfaces*, *3*(5), 1528–1537. https://doi.org/10.1021/am200102y